Kinetics of adsorption and photocatalytic decomposition of a diazo dye by nanocomposite ZnO−MgO

© *D.V. Bulyga* [1] *, S.K. Evstropiev* [1,2,3]

[1] ITMO University,
197101 St. Petersburg, Russia
[2] St. Petersburg State Technological Institute (Technical University),
190013 St. Petersburg, Russia
[3] RPA „Vavilov State Optical Institute",
St. Petersburg, Russia

e-mail: dmbulyga@yandex.ru

The synthesis of ZnO−MgO nanocomposite via modified Pechini method was performed. The crystalline structure and the morphology of nanocrystals were studied by X-ray diffraction analysis and scanning electron microscopy. The study on the kinetics of diazo dye adsorption and its photocatalytic decomposition on the surface of nanocomposite was performed. It was shown that the rate of adsorption process in aqueous solution is described by a kinetic equation of the first order. The application of the nanocomposite allows to significantly increase the efficiency of UV water treatment and its purification from the dye. However, a brief deviation of experimental data on the rate of photocatalytic degradation from the values of the widely used kinetic equation of the first order is observed.

Keywords: photocatalysis, adsorption, ZnO-MgO, nanocomposite, kinetics.

Introduction

Pollution of water environments is one of the main environmental problems on a global scale. In the problem of purification of aqueous media, various approaches can be used, such as precipitation, ozonation, adsorption, ion exchange [1]. Photocatalytic decomposition of organic pollutants is one of the most promising methods for purification of aqueous media, as it allows decomposing organic substances to inorganic oxides (H_2O, CO_2).

Under the action of UV radiation in some semiconductor oxides (ZnO, TiO_2), the process of generation of reactive oxygen species (including free radicals) occurs, which have high chemical activity and easily react with organic pollutants [2,3]. Zinc oxide, in addition to making scintillators, is also used as an antibacterial and fungicide agent [4,5].

The process of generation of reactive oxygen species occurs on the material surface; therefore, the use of semiconductor ZnO nanoparticles allows to increase the efficiency of photodecomposition of pollutants. Modification of the properties of nanocrystalline ZnO, such as the band gap and absorption spectrum, can be carried out by introducing the dopants into the material structure [6–8].

The presence of structural defects also has a significant effect on the optical, electrical, and photocatalytic properties of ZnO [9,10]. Zinc oxide is characterized by such structural defects as oxygen vacancies (V_o), interlattice zinc (Zn_i), and hydrogen (H_i) [11,12]. A controlled change in the concentration of defects allows to obtain a material with new properties, for example, with increased absorption in the visible part of the spectrum or with *n*-type conductivity.

Many applications, such as the sintering of ZnO-based ceramics, require heat treatment of the material at high temperatures. However, upon heating, structural defects in pure ZnO disappear, which can lead to a change in the properties of the material. The introduction of the dopants during the synthesis of the material allows to obtain defects in the ZnO structure, which have a higher temperature stability [13,14]. Ions with larger or smaller ionic radius replace Zn^{2+} in the ZnO structure, which leads to crystal lattice distortion and the formation of structural defects with high thermal stability.

Nanocrystalline powders can be obtained by hydrothermal synthesis [15], polymer-salt method [16] or sol-gel method [17]. The properties of the resulting material depend on the synthesis method. The modified Pechini method is a variation of the sol-gel method. The synthesis of Gd_2O_3 nanocrystalline powder using this method was described in [18]. In the synthesis of nanomaterials by the modified Pechini method, citric acid is used as a chelating agent, polyvinylpyrrolidone (PVP) plays the role of a stabilizer, as well as an organic fuel that increases the dispersion of the synthesized material due to the release of a large volume of gaseous reaction products during heat treatment. The main difference between the proposed method and the classical Pechini method is the absence of ethylene glycol in the composition of the initial solutions, as well as the presence

Chemical composition of the initial solution

Magnesium nitrate	Zinc nitrate	PVP	Citric acid	Water
0.42%	2.38%	2.27%	2.27%	92.66%

of a water-soluble polymer (PVP), which plays the role of a second stabilizer along with citric acid.

The objectives of this study are the synthesis of a nanocrystalline ZnO−MgO powder containing structural defects modified by the Pechini method and the study of the adsorption and photocatalytic properties of the obtained material.

Materials and methods

Chemical composition of the initial solution is given in the table. The concentration of magnesium oxide in the final product (ZnO−MgO) is 10 mass%. Zinc nitrate hexahydrate (chemically pure, Lenreaktiv), magnesium nitrate hexahydrate (chemically pure, Lenreaktiv), citric acid (chemically pure, Lenreaktiv), PVP, and distilled deionized water were used as initial reagents.

The masses of zinc and magnesium nitrates, calculated to obtain 25 g of the final product, were dissolved in 50 ml of water, 5 g of PVP were dissolved in 100 ml of water, 5 g of citric acid — in 50 ml of water. Then the solutions of PVP and citric acid were added to the salt solution, the resulting mixture was heated to 70°C and kept at this temperature while stirring with a magnetic stirrer. The resulting solution was dried at a temperature of 70°C in an oven, the resulting polymer-salt composition was subjected to heat treatment at a temperature of 550°C for 2 h in an electric muffle furnace with a hood.

X-ray diffraction patterns of the synthesized powder were obtained using a Rigaku Ultima IV X-ray diffractometer, the morphology of powder particles was studied using Tesla BS-301 scanning electron microscope.

The study of the adsorption activity of the synthesized powder was carried out as follows. Into a quartz cuvette with 3 ml of Chicago Sky Blue (CGB) organic dye solution, 20 mg of the test powder were placed. The content of the dye in the initial solutions was 9 mg/l. This dye was used earlier in [19–23] to evaluate the photocatalytic properties of materials. In aqueous dye solutions, an intense absorption band with a maximum of $\lambda_{max} = 612$ nm is observed. In [24] the experimentally determined dependence of the optical density of CSB aqueous solutions at this wavelength on the dye concentration was given. In the present study, this dependence was used to determine the concentration of the dye in the studied solutions.

Then, using a spectrophotometer, absorption spectra were recorded with a time interval of 7.5 min (taking into account the measurement time). Using the calibration curve (the dependence of the optical density of the
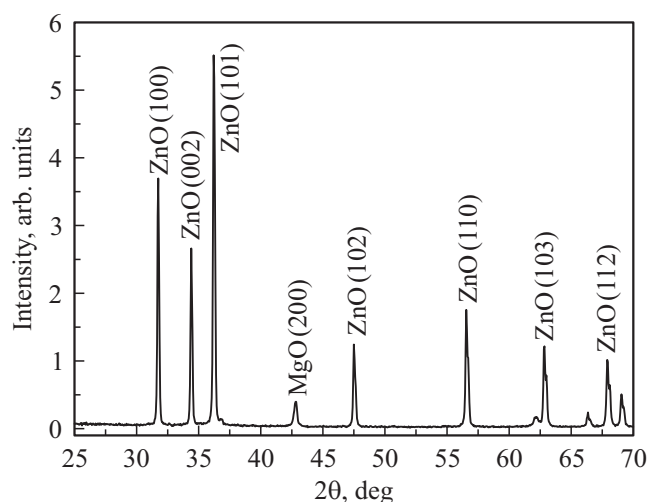
Figure 1. X-ray diffraction pattern of ZnO−MgO powder.

solution on the concentration of the dye), according to the Bouguer−Lambert−Beer law, the change in concentration during the adsorption of the dye by the powder was calculated. Based on the data obtained, a time dependence of the change in the concentration of the solution (kinetic curve) was constructed.

The study of photocatalytic activity was carried out by a similar method. A quartz cell with a dye solution and powder was irradiated for 5 min with UV radiation, and the absorption spectra were recorded for 2.5 min. On the basis of the data obtained, a kinetic curve for the photocatalytic decomposition of the dye in solution was plotted.

The absorption spectra were recorded using Perkin Elmer Lambda 650 UV/VIS spectrophotometer; a mercury lamp was used as a source of UV radiation.

The luminescence spectra of the synthesized materials were recorded using Perkin Elmer LS50B spectrofluorimeter.

Experimental results and discussion

Structure and morphology of ZnO−MgO powder particles

The X-ray diffraction pattern of the ZnO−MgO powder is given in the Fig. 1. Most of the observed peaks belong to the ZnO phase, one weak peak corresponds to the magnesium oxide phase, which indicates the formation of a small amount of this substance.

The average size of nanocrystals was calculated using the Scherrer formula (1):

$$D = \frac{K\lambda}{B\cos\chi},\qquad(1)$$

where D — average size of nanocrystals, K — constant depending on particle shape, B width at half maximum of
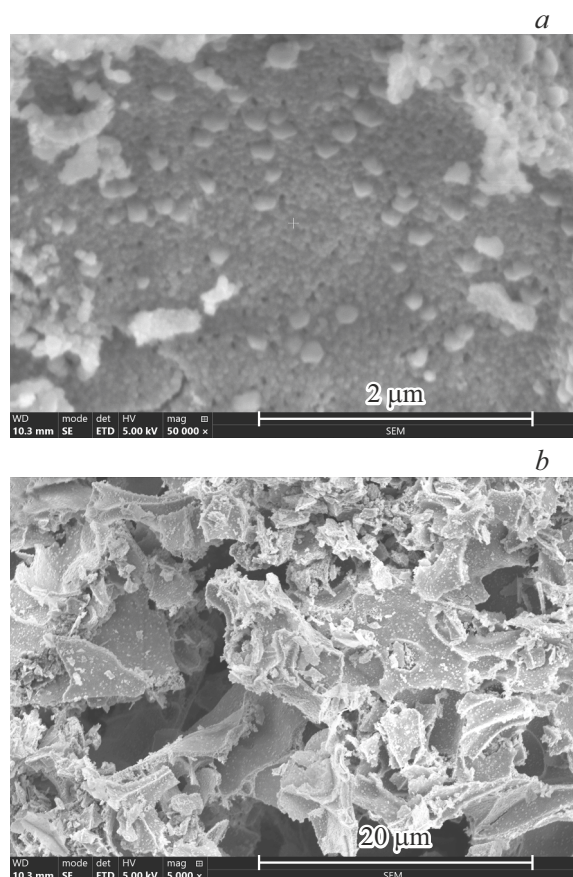
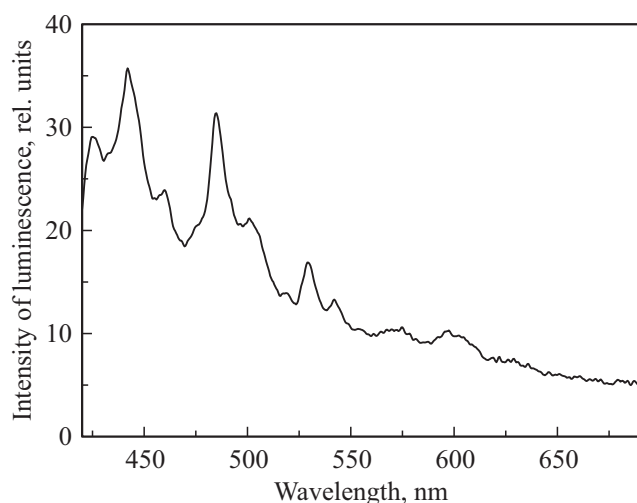**Figure 2.** SEM-images of powder ZnO−MgO particles.

Figure 3. Luminescence spectrum of the ZnO−MgO nanocomposite.

the most intense peak, χ — Bragg angle [25]. According to calculations, the average size of nanocrystals is 78ṅm.

SEM images of particles of the synthesized powder are shown in Fig. 2.

According to the SEM data, the synthesized powder consists of the aggregated nanoparticles 70−150 nm in size.

Considering that most of the nanoparticles have sizes of the order of 70−90 nm, the result obtained agrees with the data obtained by calculation using the Scherrer formula.

Luminescent properties of the ZnO−MgO nanocomposite

The luminescence spectrum of the synthesized ZnO−MgO nanocomposite is shown in Fig. 3. The excitation wavelength is 370 nm.

The luminescence spectrum consists of an exciton band in the UV part of the spectrum and bands in the visible part of the spectrum, corresponding to structural defects typical of zinc oxide. The effect of the surface defects on the luminescence spectrum is especially pronounced in nanocrystalline ZnO due to the high specific surface area [10,26]. The luminescence bands with maxima near 415, 440 and 455 nm correspond to interlattice zinc [27], the bands in the spectral region 510−600 nm correspond to oxygen vacancies [10,28].

Adsorption and photocatalytic activity

Figure 4 shows the data illustrating the change in the absorption spectra of aqueous solutions of the dye during its adsorption by the nanocomposite (*a*), during its photodecomposition in solution (*b*) and during its photocatalytic decomposition (*c*). It can be seen that in all cases no change in the shape of its absorption spectra is observed, and the most rapid and significant changes in the spectra of solutions are observed during the photocatalytic decomposition of the dye (Fig. 4, *c*).

Data on changes in the relative concentration of the dye during its photodecomposition in solution (curve *1*), during its adsorption on the surface of nanocomposite particles (curve *2*), and during photocatalytic decomposition are shown in Fig. 5. The calculated curves $C/C_0 = f(t)$ corresponding to changes in the relative concentration in accordance with equation (2) are also shown in this figure.

The rate of discoloration of the solution during the photocatalytic process is determined by the combined action of several main processes:

1) photodecomposition of the dye in the liquid phase,

2) dye adsorption on the photocatalyst surface,

3) photocatalytic decomposition of dye molecules adsorbed on the surface of photocatalyst particles.

Processes 2 and 3 are sequential, and the photodecomposition of the dye in the liquid phase proceeds independently and simultaneously with processes 2 and 3.

Kinetics of dye photolysis in the liquid phase

For a formal description of the photodecomposition kinetics of various organic substances, the first-order kinetic equation is widely used [29–38]
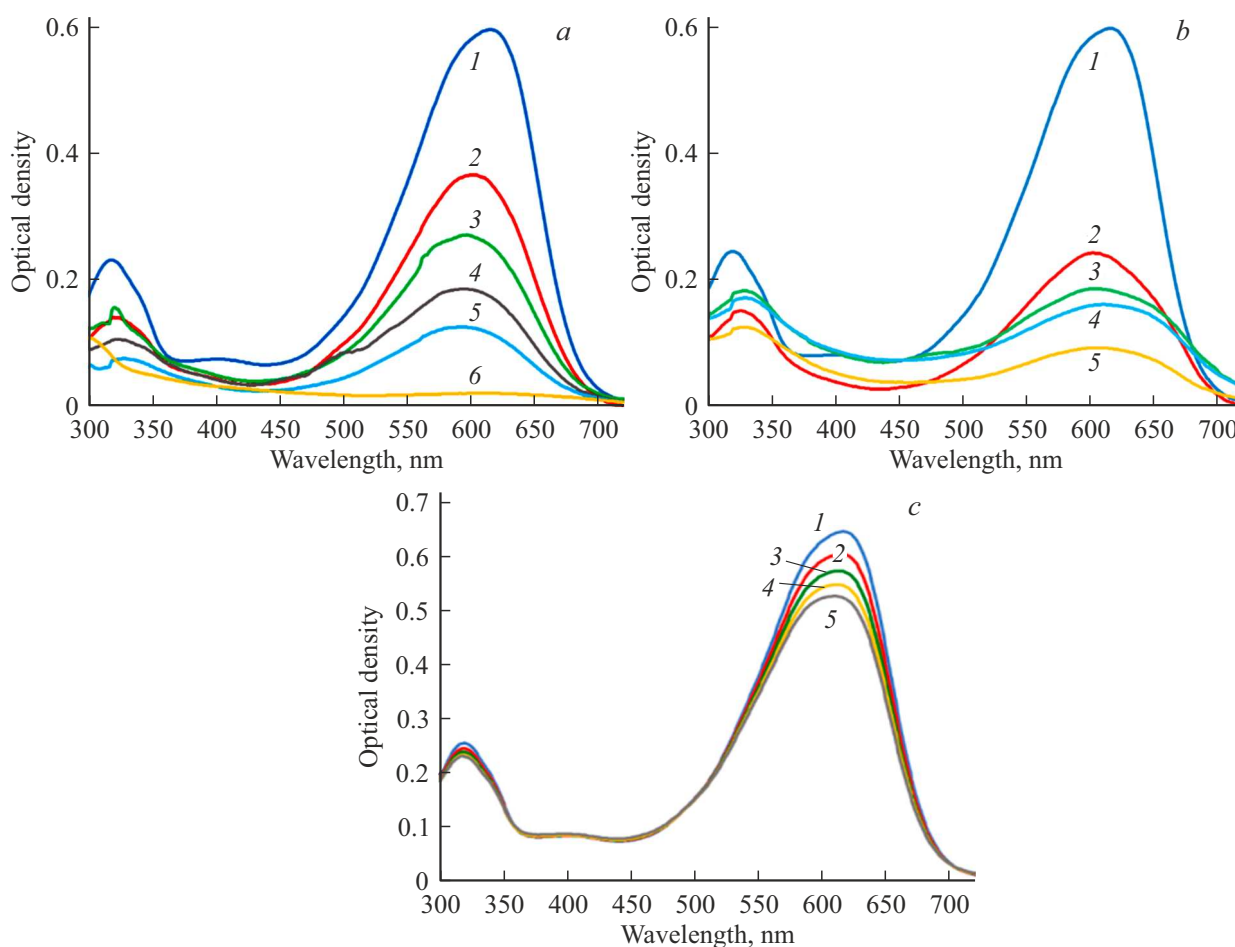
$$-\frac{dc}{dt} = kc, \qquad (2)$$

Figure 4. Changes in the absorption spectra of aqueous solutions of the dye during its adsorption by the nanocomposite (*a*), photodecomposition (*b*), and photocatalytic decomposition (*c*). Duration of *a* and *c* processes: initial solution (curves *1*), 7.75 (curves *2*), 15.50 (curves *3*), 23.25 (curves *4*), 31.00 (curves *5*), 2880.00 min (curve *6*). Process duration for photodecomposition in solution: initial solution (curve *1*), 5 (curve *2*), 10 (curve *3*), 15 (curve *4*), 20 min (curve *5*).

which after integration is as follows

$$\frac{C}{C_0} = e^{-kt}, \qquad (3)$$

where C_0 and C — initial and current dye concentrations (mM), t — duration of the irradiation process (min) and k — reaction rate constant (min^{-1}).

To a certain extent, the basis for applying equations (2) and (3) can be the basic law of photochemical kinetics, which can be expressed by the equation [39]

$$-\frac{\partial C}{C}\frac{1}{\partial t} = K\frac{1}{h\nu^2} \qquad (4)$$

where I — intensity of incident light, $h\nu$ — photon energy, C — concentration of dye molecules, K — photosensitivity of the given system. When a stable radiation source is used in the experiment, the value of $I/h\nu$ on the right side of equation (3) is constant, and the dye concentration changes exponentially during the photochemical reaction.

Figure 6 shows the graph of the dependence $\ln(C/C_0) = f(t)$ for the photodecomposition of the dye in solution. The experimental data are well described by a linear dependence with the coefficient of determination $R^2 = 0.996$. This indicates the adequacy of the kinetic model, which expresses the change in the photodecomposition rate of the dye in solution by a first-order equation.

Adsorption kinetics

The kinetics of the processes of adsorption of organic substances from solutions on the surface of solid materials has been the subject of research for many years. To date, many kinetic models have been proposed that take into account individual features of the processes to one degree or another and describe specific experimental data with varying accuracy [39–46]. The adequacy of the description of experimental data by kinetic models is estimated by the value of the coefficient of determination R^2 [46]. Among the kinetic models of adsorption most frequently used in
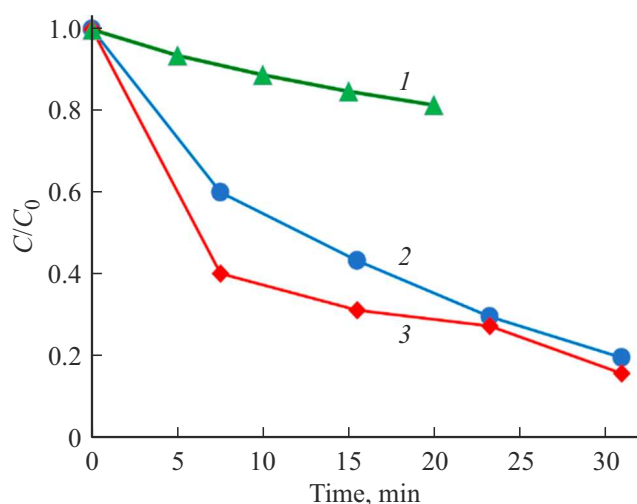
Figure 5. Dependences of the relative concentration of the dye during its photodecomposition in solution (curve *1*), during its adsorption on the surface of nanocomposite particles (curve *2*), and during photocatalytic decomposition (curve *3*).
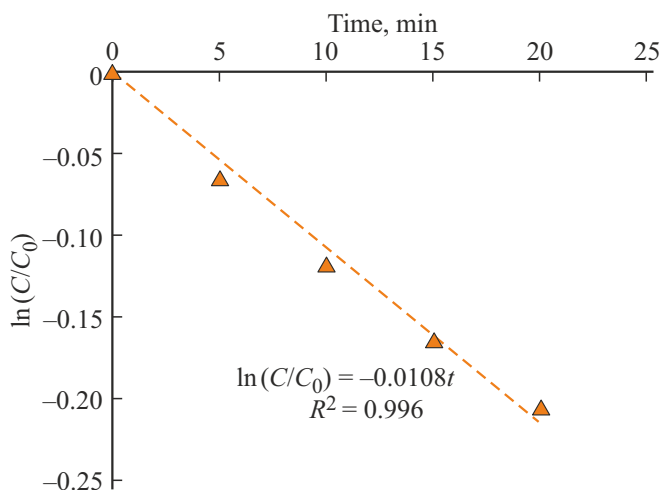

Figure 6. Graph of dependence $\ln(C/C_0) = f(t)$ for the process of dye photodecomposition in solution.

describing the rate of photocatalytic processes, one can single out pseudo-first and pseudo-second order models.

Figure 5 (curve *1*) shows the dependence of the relative dye concentration in the suspension on the duration of the process of adsorption by the ZnO−MgO powder. It can be seen that the strongest change in concentration occurs during the first 10−15 min of the process, and then the adsorption rate decreases significantly.

The pseudo-first-order kinetic equation proposed by Lagergren [39,45] and describing the process of adsorption on the surface of solids can be written as [39,40,45]

$$\frac{dq_t}{dt} = k_f(q_e - q_t), \qquad (5)$$

where q_t (mM/g) — is the amount of dye adsorbed by 1 g of the sorbent by time t, q_e – is the equilibrium adsorption capacity of the sorbent, k_f (min^{-1}) — adsorption rate constant, t — duration of adsorption process (min). It can be seen from the equation that as the surface is filled with dye molecules, the adsorption rate decreases.

Figure 7 shows the dependence $\ln(q_e - q_t) = f(t)$ constructed on the basis of experimental results. It can be seen that this dependence is close to linear, which allows us to conclude that the adsorption rate of the diazo dye on the surface of the ZnO−MgO nanocomposite is well described by the kinetic equation (5). The obtained value of the coefficient of determination $R_2 = 0.9954$ indicates a good agreement between the pseudo-first-order adsorption kinetic model and the experimental values.

The value of the adsorption rate constant $(k_f = 0.0558 \, \text{min}^{-1})$ determined using the graph $\ln(q_e - q_t) = f(t)$ (Fig. 7, *a*) is quite large. Similar values of k_f were observed earlier in [47] for the adsorption rate of the methylene blue dye on ZnO nanoparticles.

Also, the pseudo-second order equation is often used to describe the adsorption kinetics

$$\frac{dq_t}{dt} = k_2(q_e - q_t)^2, \qquad (6)$$

which can be written in integrated form [48–51,43,44]

$$\frac{t}{q_t} = \frac{1}{k_2 q_e^2} + \frac{t}{q_e}, \qquad (7)$$

where k_2 — is the second-order adsorption rate constant, q_e — is the maximum equilibrium adsorption capacity of the photocatalyst (mg/g), q_t — the content of the adsorbed dye on the surface of the photocatalyst at time t (mg/g). This model describes a much stronger dependence of the adsorption rate on the degree of coverage of the surface of a solid material with dye molecules. The graph $\frac{t}{q_t} = f(t)$ showed satisfactory agreement between the experimental data and equation (7) (Fig. 7, *b*). However, the value of the coefficient of determination R^2 was 0.9895, which is less than that obtained for the pseudo-first-order kinetic model (Fig. 7, *a*).

Thus, we can conclude that the pseudo-first-order adsorption kinetic model describes the obtained experimental data somewhat better.

Kinetics of photocatalytic dye decomposition

The photodecomposition kinetics of azo dyes is usually described by the Langmuir−Hinshelwood model and approximated by the kinetic equation [52,53]

$$-\frac{dC}{dt} = k_1 K_a C 1 + K_a C, \qquad (8)$$

where C — current concentration of the dye at time t, k_1 — process rate constant, K_a — adsorption equilibrium constant.
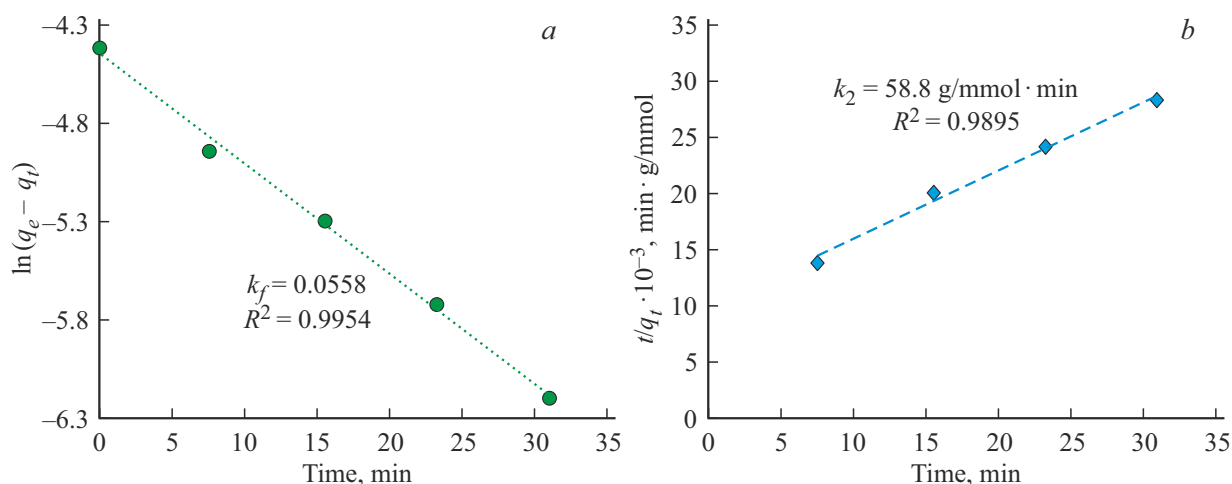
Figure 7. Dependencies: (*a*) $\ln(q_e - q_t) = f(t)$ and (*b*) $t/q_t = f(t)$.
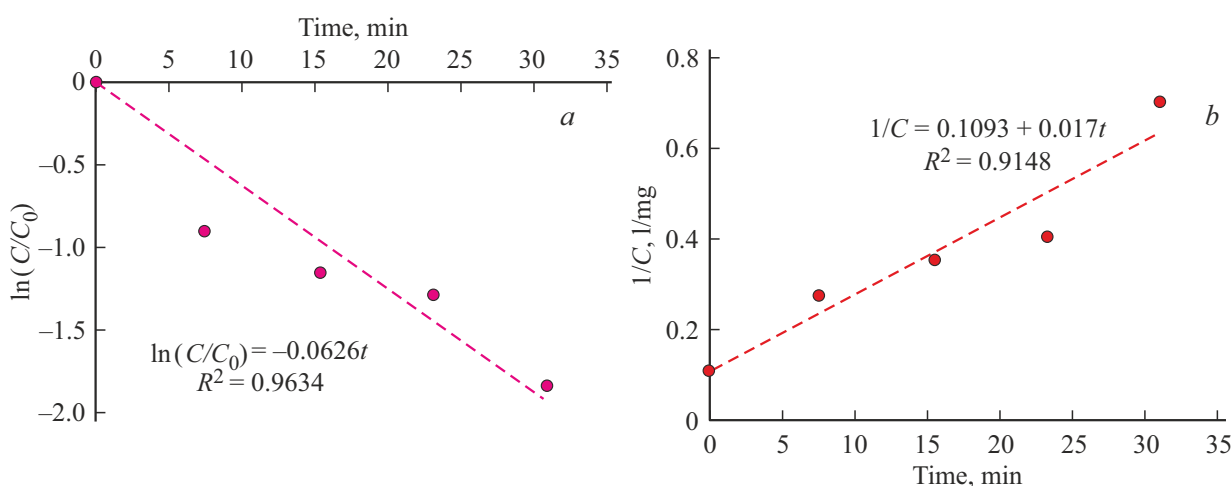

Figure 8. Dependency diagram $\ln(C/C_0) = f(t)$ (*a*) and $1/C = f(t)$ (*b*).

At a low dye concentration ($C \ll 1\,\text{mM}$), equation (8) simplifies to a pseudo-first-order process rate equation [53,54]

$$\ln(C/C_0) = k_1 K_a t = k_{app} t, \qquad (9)$$

where k_{app} — pseudo first order rate constant.

Figure 8, *a* shows the graph of the dependence $\ln(C/C_0) = f(t)$, built on the basis of experimental data. It can be seen that the linear dependence corresponds to these data with the coefficient of determination $R_2 = 0.9634$, which is close to similar literature data [31,47,55]. It can be noted that the obtained value $k_{app} = 0.062\,\text{min}^{-1}$ somewhat exceeds the rate constant of photodecomposition of methylene blue dye on ZnO:Cr nanorods ($0.043\,\text{min}^{-1}$), synthesized and studied in [56].

The equation used in the kinetic model for pseudo-second order photocatalysis can be written as [47]

$$\frac{1}{C} = \frac{1}{C_0} + k_2 t, \qquad (10)$$

where k_2 — is the rate constant of the pseudo-second order photocatalytic reaction. Figure 8, *b* shows the plot of $1/C = f(t)$, from which it can be seen that this kinetic model is worse (compared to the pseudo-first order model) in agreement with the experimental data, and the value of the coefficient of determination is relatively small ($R_2 = 0.9148$).

It should be noted that the deviations of the experimental results from the data obtained using the pseudo-first and pseudo-second order photodecomposition kinetic models are quite significant (Fig. 8).

According to [24], the change in the Gibbs free energy ΔG_{ad} upon adsorption of CSB from solution onto the surface of ZnO−Ag nanoparticles is $-26\,\text{kJ/mol}$, which is close to the change in ΔG_{dim} during dimerization of this dye molecules in solutions ($-28\,\text{kJ/mol}$ ([57]). The closeness of these values determines the possibility of polymolecular („multilayer") adsorption occurring simultaneously with the formation of the first layer of dye molecules adsorbed
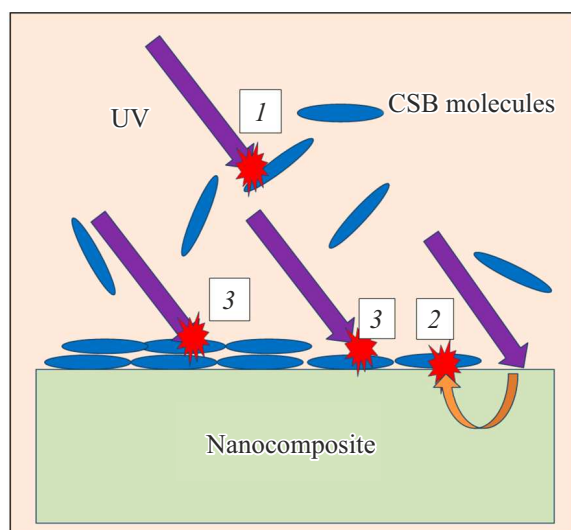
Figure 9. Illustrative scheme of dye photodecomposition: *1 —* photolysis of dye molecules in solution, *2 —* photocatalytic decomposition of the dye on the nanocomposite surface, *3 —* photolysis of adsorbed dye molecules.

on the surface of the nanocomposite. The possibility of polymolecular adsorption of organic dyes on the surface of solid oxide materials is described in the literature ([58]).

At a high adsorption rate, the layers of adsorbed dye molecules formed on the surface of the nanocomposite shield the semiconductor material from external radiation, reducing the efficiency of photocatalysis. Figure 9 shows an illustrative scheme of this process. According to this scheme, dye molecules undergo photodecomposition:

a) in solution (process 1, Fig. 9); the decomposition rate of these molecules is well described by equations (1) and (2),

b) adsorbed on the surface of the composite and oxidized by reactive oxygen species released by the semiconductor composite under the action of external radiation (process 2, Fig. 9).

c) adsorbed on the surface of the composite and decomposed by direct exposure to UV radiation (process 3, Fig. 9). The rates of processes 1 and 3 of dye photolysis without the participation of a photocatalyst are close. These photochemical reactions proceed relatively slowly (Fig. 5 (curve *1*) and Fig. 6).

At the initial stages of the solution bleaching process (the first 5?10 min of irradiation, Fig. 5), the concentration of CSB molecules adsorbed on the surface of the composite is low, their screening effect is small, and a significant contribution to the photodecomposition of the dye is made by the photocatalytic mechanism characterized by a relatively high rate and efficiency. However, as the adsorption process proceeds, the screening effect of the layer of adsorbed molecules increases, and the fast photocatalytic mechanism of dye decomposition is replaced by a much slower photolysis of adsorbed molecules. The rate of

discoloration of the solution then decreases and approaches the rate of adsorption of dye molecules (irradiation duration 20−40 min, Fig. 5). The proposed scheme allows to explain the observed discrepancy between the experimental data and the known and most commonly used models of photocatalysis kinetics.

Conclusion

Based on the consideration of the features of the formation of structural defects in zinc oxide and their significant effect on its photocatalytic properties, we chose the chemical composition of a ZnO-based solid solution modified with Mg^{2+} ions and including the corresponding defects in the crystal structure. The ZnO−MgO nanocomposite was synthesized by the modified Pechini method, and its morphology and structure were studied by X-ray phase analysis and scanning electron microscopy. The study of the luminescence spectra of the composite in the visible part of the spectrum confirmed the presence of characteristic structural defects in zinc oxide.

The study of the kinetics of the processes of adsorption and photocatalytic decomposition of the CSB diazo dye showed that the synthesized nanocomposite has a high efficiency and rate of dye removal from solutions. Experimental data are satisfactorily described by pseudo-first-order kinetic models of the rate of processes.

Conflict of interest

The authors declare that they have no conflict of interest.

References

[1] *Organic Pollutants−Monitoring, Risk and Treatment*, ed. by M. Nageeb (InTech, Rijeka, Croatia, 2013).

[2] X. Chen, Z. Wu, D. Liu, Z. Gao. Nanoscale Res. Lett., **12** (1), 1 (2017). DOI: 10.1186/s11671-017-1904-4

[3] S.-Y. Lee, S.-J. Park. J. Industrial and Engineering Chemistry, **19** (6), 1761 (2013). DOI: 10.1016/j.jiec.2013.07.012

[4] C. Karunakaran, V. Rajeswari, P. Gomathisankar. Solid State Sciences, **13** (5), 923 (2011).
DOI: 10.1016/j.solidstatesciences.2011.02.016

[5] A. Sierra-Fernandez, S.C. De la Rosa-García, L.S. Gómez-Villaba, S. Gómez-Cornelio, M.E. Rabanal, P. Quintana. ACS Appl. Mater. Interfaces, **9** (29), 24873 (2017).
DOI: 10.1021/acsami.7b06130

[6] R. Saravanan, N. Karthikeyan, S. Govindan. Advanced Materials Research, **584**, 381 (2012).
DOI: 10.4028/www.scientific.net/AMR.584.381

[7] S. Yadav, A. Mittal, S. Sharma. Semiconductor Science and Technology, **35**, 055008 (2020).
DOI: 10.1088/1361-6641/ab7776

[8] M. Zhang, G. Sheng, J. Fu, T. An, X. Wang, X. Hu. Materials Lett., **59**, 3641 (2005). DOI: 10.1016/j.matlet.2005.06.037

[9] L. Zheng, M. Liu, H. Zhang, Z. Zheng, Z. Wang, H. Cheng, P. Wang, Y. Liu, B. Huang, Nanomaterials, **11** (10), 2506 (2021). DOI: 10.3390/nano11102506

[10] P.A. Rodnyi, K.A. Chernenko, I.D. Venevtsev. Opt. Spectrosc., **125**, 372 (2018).

[11] J.P. Wang, Z.Y. Wang, B.B. Huang, Y.D. Ma, Y.Y. Liu, X.Y. Zhang, Y. Dai. ACS Appl. Mater. Interfaces, **4**, 4024 (2012).

[12] L.S. Liu, Z.X. Mei, A.H. Tang, A. Azarov, A. Kuznetsov, Q.K. Xue, X.L. Du. Phys. Rev. B, **93**, 235305 (2016). DOI: 10.1103/PhysRevB.93.235305

[13] A.A. Shelemanov, S.K. Evstropiev, A.V. Karavaeva, N.V. Nikonorov, V.N. Vasilyev, Y.F. Podruhin, V.M. Kiselev. Mater. Chem. Phys., **276**, 125204 (2022). DOI: 10.1016/j.matchemphys.2021.125204

[14] V.E. Etacheri, R. Roshan, V. Kumar. ACS Appl. Mater. Interfaced, **4** (5), 2717 (2012). DOI: 10.1021/am300359h

[15] A.N.P. Madathil, K.A. Vanaja, M.K. Jayaraj. Intern. Society for Optics and Photonics, **6639**, 66390J (2007). DOI: 10.1117/12.730364

[16] A.A. Shelemanov, S.K. Evstropiev, V.M. Kiselev, N.V. Nikonorov. Opt. Spectrosc., **129**, 1300 (2021). DOI: 10.1134/S0030400X21090198

[17] J.N. Hasnidawani, H.N. Azlina, H. Norita, N.N. Bonnia, S. Ratim, E.S. Ali. Procedia Chemistry, **19**, 211 (2016). DOI: 10.1016/j.proche.2016.03.095

[18] A. Moussaoui, D.V. Bulyga, S.K. Evstropiev, A.I. Ignatiev, N.V. Nikonorov, Y.F. Podruhin, R.V. Sadovnichii. Ceramics International, **47** (24). 34307 (2021). DOI: 10.1016/j.ceramint.2021.08.341

[19] S.K. Evstropiev, V.N. Vasilyev, N.V. Nikonorov, E.V. Kolobkova, N.A. Volkova, I.A. Boltenkov. Chemical Engineering and Processing: Process Intensification, **134**, 45 (2018). DOI: 10.1016/j.cep.2018.10.020

[20] I.S. Boltenkov, E.V. Kolobkova, S.K. Evstropiev. J. Photochem. and Photobiol. A: Chemistry, **367**, 458 (2018). DOI: 10.106/j.photochem.2018.09.016

[21] S.K. Evstropiev, L.V. Lesnykh, A.V. Karavaeva, N.V. Nikonorov, K.V. Oreshkina, L.Yu. Mironov, S.Yu. Maslennikov, E.V. Kolobkova, I.V. Bagrov. Chemical Engineering and Processing: Process Intensification, 142, 107587 (2019). DOI: 10.1016/j.cep.2019.107587

[22] N.A. Volkova, S.K. Evstropiev, O.V. Istomina, E.V. Kolobkova. Opt. Spectrosc., **124** (4), 489 (2018).

[23] S. Noreen, U. Khalid, S.M. Ibrahim, T. Javed, A. Ghani, S. Naz, M. Iqbal. J. Materials Research and Technology, **9** (3), 5881 (2020). DOI: 10.1016/j.jmrt.2020.03.115

[24] A.S. Saratovskii, D.V. Bulyga, S.K. Evstrop'ev, T.V. Antropova. Physics and Chemistry, **48** (1), 10 (2022). DOI: 10.1134/S1087659622010126

[25] A.L. Patterson. Phys. Rev., 56 (10), 978 (1939).

[26] H. Zeng, G. Duan, Y. Li, S. Yang, X. Xu, W. Cai. Advanced Functional Materials, **20** (4), 561 (2010). DOI: 10.1002/adfm.200901884

[27] S. Vempati, J. Mitra, P. Dawson. Nanoscale Research Lett., **7** (1), 1(2012).

[28] D. Das, P. Mondal. RSC Adv., **4**, 35735 (2014). DOI: 10.1039/C4RA06063F

[29] G. Liao, W. He, Y. He. Catalysts, **9**, 502 (2019). DOI:10.3390/catal9060502

[30] J. Araña, J.L. Martínez Nieto, J.A. Herrera Melián, J.M. Doña Rodríguez, O. González Díaz, J. Pérez Peña, O. Bergasa, C. Alvarez, J. M?ndez. Chemosphere, **55** (6), 893 (2004). DOI: 10.1016/j.chemosphere.2003.11.060Get

[31] X. Chen, Z. Wu, D. Liu, Z. Gao. Nanoscale Res. Lett., **12**, 143(2017).

[32] E.J. Wolfrum, J. Huang, D.M. Blake, P.C. Maness, Z. Huang, J. Fiest, W.A. Jacoby, Environ. Sci. Technol., **36** (5), 3412 (2002). DOI: 10.1021/es011423

[33] I.S. Boltenkov, E.V. Kolobkova, S.K. Evstropiev. J. Photochem. and Photobiol. A: Chemistry, **367**, 458 (2018). DOI: 10.106/j.photochem.2018.09.016

[34] I.A. Majeed, W.J. Murray, D.W. Newton, S. Othman, W.A. A-Turk, J. Pharm. Pharmacol., **39** (12), 1044 (1987). DOI: 10.1111/j.2042-7158.1987.tb03160.x

[35] V.V. Venkata, P.H. Sadashivaiah. Europ. J. Chem., **3** (2), 191 (2012). DOI: 10.5155/eurjchem.3.2.191-195.564

[36] M.A. Johar, R.A. Afzal, A.A. Alazba, U. Manzoor Advances in Materials Science and Engineering, 2015, 934587 (2015). DOI: 10.1155/2015/934587

[37] S.K. Evstropiev, L.V. Lesnykh, A.V. Karavaeva, N.V. Nikonorov, K.V. Oreshkina, L.Yu. Mironov, S.Yu. Maslennikov, E.V. Kolobkova, I.V. Bagrov. Chemical Engineering and Processing: Process Intensification, **142**, 107587 (2019). DOI: https://doi.org/10.1016/j.cep.2019.107587

[38] Z. Cheng, S. Zhao, L. Han. Nanoscale, **10**, 6892 (2018). DOI: 10.1039/c7nr09683f

[39] A.N. Terenin. Fotokhimiya krasiteley i rodstvennykh organicheskikh soedineniy (Nauka, M., 1967), p. 101. (in Russian).

[40] S. Lagergren. Kungliga Sevenska Vetenskapasakademiens Handlingar, **24**, 1 (1898).

[41] S. Kaur, S. Rani, R.K. Mahajan. J. Chemistry, **2013**, 628582 (2013). DOI: 10.1155/2013/628582

[42] M.J. Weber, J. Morris. ASCE J. Saint Engineering Division, **89**, 31 (1963). DOI: 10.1061/JSEDAI.0000430

[43] Y.S. Ho, G. McKay. Process Saf. Environ. Protect, **76B.**, 183 (1998). DOI: 10.1205/095758298529326

[44] Y.S. Ho, G. McKay. Process Safety and Environmental Protection, **76**, 332 (1998). DOI: 10.1205/095758298529696

[45] S. Lagergren. Kungliga Sevenska Vetenskapasakademiens Handlingar, **24**, 39 (1898).

[46] O.O. Kryzhanovskaya, L.A. Sinyaeva, S.I. Karpov, V.F. Selemenev, E.V. Borodina, F. Ryossner. Sorbcionnye i hromatograficheskiye processy, **14** (5), 784 (2014). (in Russian).

[47] M. Irani, T. Mohammadi, S. Mohebbi. J. Mex. Chem. Soc., **60** (4), 218 (2016).

[48] Y.-S. Ho, J. Hazard. Mater., **136** (3), 681 (2006). DOI: 10.1016/j.jhazmat.2005.12.043

[49] Y. Kuang, X. Zhang, S. Zhou. Water, **12**, 587 (2020). DOI: 10.3390/w12020587

[50] J. P. Simonin. Chem. Eng. J., **300**, 254 (2016). DOI:10.1016/j.cej.2016.04.079

[51] J.C. Bullen, S. Sleesongsom, K. Gallagher, D.J. Weiss. Langmuir, **37** (10), 3189 (2021). DOI: 10.1021/acs.langmuir.1c00142

[52] V.I. Gaya, A.H. Abdullah, J. Photochem. Photobiol. C: Photochem. Rev., **9**, 1 (2008). DOI: 10.1016/j.jphotochemrev.2007.12.003

[53] I.K. Konstantinou, T. A. Albanis. Appl. Catalysis B: Environmental, **49** (1), 1 (2004).
DOI: 10.1016/j.apcatb.2003.11.010

[54] V. Vimonses, M.N. Chong, B. Jin. Microporous and Mesoporous Materials, **132**, 201 (2010).
DOI: 10.1016/j.micromeso.2010.02.021

[55] W. Liu, T. He, U. Wang, G. Ning, Z. Xu, X. Chen, X. Hu, Y. Wu, Y. Zhao. Sci. Rep., **10**, 11903 (2020).
DOI: 10.1038/s4158-020-68517-x

[56] J. Chen, Y. Xiong, M. Duan, X. Li, J. Li, S. Fang, S. Qin, R. Zhang. Langmuir, **36** (2), 520 (2020).
DOI: 10.1021/acs.langmuir.9b02879

[57] L.C. Abbott, S.N. Batchelor, J. Oakes, J.R. Lindsay Smith, J.N. Moore. J. Phys. Chem. B, **108**, 13786 (2004).

[58] N.R. Senatorova, B.D. Ryzhikov. Vestnik Moskovskogo universiteta. Series 3. Fizika. Astronomiya, **29** (1), 43 (1988) (in Russian).